



Motorized Macrocyclic Host with Switchable and Stereoselective Guest Recognition

Yue Liu⁺, Qi Zhang⁺, Stefano Crespi, Shaoyu Chen, Xiu-Kang Zhang, Tian-Yi Xu, Chang-Shun Ma, Shang-Wu Zhou, Zhao-Tao Shi, He Tian, Ben L. Feringa,* and Da-Hui Qu*

Abstract: Designing photo-responsive host–guest systems can provide versatile supramolecular tools for constructing smart systems and materials. We designed photo-responsive macrocyclic hosts, modulated by light-driven molecular rotary motors enabling switchable chiral guest recognition. The intramolecular cyclization of the two arms of a first-generation molecular motor with flexible oligoethylene glycol chains of different lengths resulted in crown-ether-like macrocycles with intrinsic motor function. The octaethylene glycol linkage enables the successful unidirectional rotation of molecular motors, simultaneously allowing the 1:1 host–guest interaction with ammonium salt guests. The binding affinity and stereoselectivity of the motorized macrocycle can be reversibly modulated, owing to the multi-state light-driven switching of geometry and helicity of the molecular motors. This approach provides an attractive strategy to construct stimuli-responsive host–guest systems and dynamic materials.

Introduction

Since the pioneering developments in supramolecular chemistry by Cram, Lehn, and Pedersen,^[1] the design and synthesis of macrocycle-based host–guest systems have taken a prominent position at the frontiers of chemistry.^[2] Numer-

ous macrocycles have been synthesized, exhibiting reversible, selective, and high-affinity binding interactions with specific guests.^[3] These features further expanded the broad range of applications of macrocyclic host–guest systems, including the construction of artificial molecular machines, supramolecular polymers, sensors, delivery systems, separation technology, fluorescent materials, and dynamic materials.^[4] Developing host–guest systems that can respond to external stimuli is particularly attractive. Taking advantage of non-covalent bonds and intrinsic switching properties provides powerful tools for designing dynamic supramolecular systems and materials which properties and functions can be modulated on command.^[4,5]

Light is widely recognized among different stimulus modes as the ideal way to control responsive materials and systems^[6] because it benefits from being remote, instantaneous, clean, and wavelength tunable, allowing to achieve high spatial-temporal control. A general strategy of designing light-responsive host–guest systems involves the introduction of photo-isomerizing units into the structures of the macrocyclic hosts or guests, enabling the effective variation of noncovalent binding affinities by conformational transformation.^[3,4,7] Many approaches have been reported using photo-switchable azobenzenes,^[8] stilbenes,^[9] spiropyrans,^[10] and diarylethenes,^[5a,6f,11] showing their versatility in fabricating bistable photo-responsive macrocyclic receptors. However, the design and functioning of light-modulated host–guest systems with multi-stable switching possibilities remains a major challenge. Meanwhile, enabling and controlling the selectivity with different guest molecules, especially with distinct chiral guests, is critical to developing synthetic biomimetic smart host–guest systems.

Light-driven molecular motors^[12] based on overcrowded alkenes have been developed as a unique family of photo-responsive units in the last decades. Due to their intrinsic feature of performing unidirectional rotation, molecular motors have been explored as robust and versatile functional units to fabricate many photo-responsive materials, including liquid crystals,^[13] soft actuators,^[6b,14] gels,^[15] foams,^[16] membranes,^[17] solid-state surfaces,^[18] porous frameworks,^[19] and nanocars.^[20] The intrinsic axial chirality and photoswitching ability of molecular motors, resulting in multiple stable chiral states with precise control over the sequence of chiral isomer formation, are the key features of asymmetric catalysts and phosphate receptors with adaptive chirality.^[21] These fascinating applications stimulated the introduction of molecular motors into macrocyclic host–guest systems, which might give access to an intriguing family of intrinsic motorized macro-

[*] Dr. Y. Liu,^[†] Dr. Q. Zhang,^[†] Dr. S. Chen, X.-K. Zhang, T.-Y. Xu, C.-S. Ma, S.-W. Zhou, Z.-T. Shi, Prof. H. Tian, Prof. B. L. Feringa, Prof. D.-H. Qu

Key Laboratory for Advanced Materials and Joint International Research Laboratory of Precision Chemistry and Molecular Engineering, Feringa Nobel Prize Scientist Joint Research Center, Frontiers Science Center for Materiobiology and Dynamic Chemistry, Institute of Fine Chemicals, School of Chemistry and Molecular Engineering, East China University of Science and Technology Shanghai, 200237 (China)

E-mail: dahui_qu@ecust.edu.cn

Dr. Q. Zhang,^[†] Dr. S. Crespi, Dr. S. Chen, Prof. B. L. Feringa Centre for Systems Chemistry, Stratingh Institute for Chemistry and Zernike Institute for Advanced Materials, University of Groningen Nijenborgh 4, 9747 AG Groningen (The Netherlands)

E-mail: b.l.feringa@rug.nl

[†] These authors contributed equally to this work.

Supporting information and the ORCID identification number(s) for the author(s) of this article can be found under: <https://doi.org/10.1002/anie.202104285>.

© 2021 The Authors. Angewandte Chemie International Edition published by Wiley-VCH GmbH. This is an open access article under the terms of the Creative Commons Attribution License, which permits use, distribution and reproduction in any medium, provided the original work is properly cited.

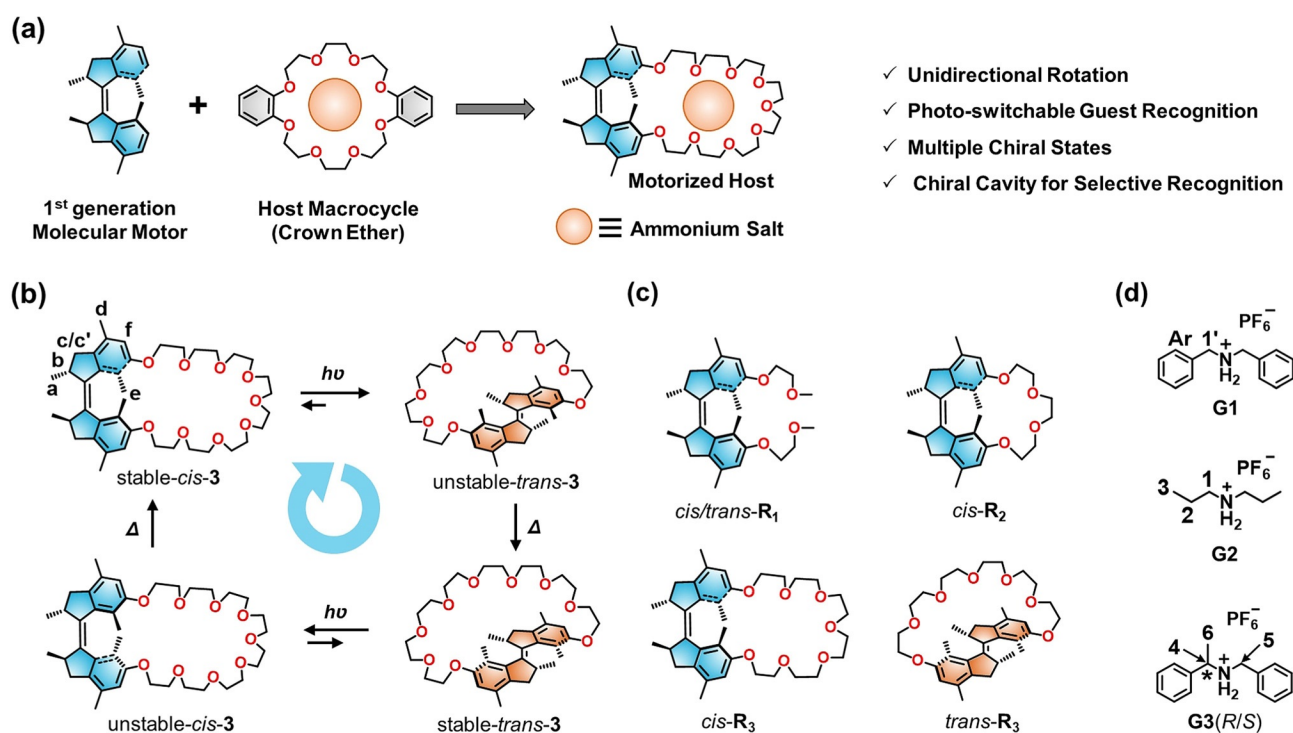


Figure 1. a) Representation of the structure of the novel motorized macrocycle. b) The rotation in an intramolecular confined space of motorized macrocycle **3**. c) Reference compounds. d) Guest molecules.

cycles that can dynamically modulate their guest binding ability and chiral recognition by unidirectional rotation.

Here we report the combination of molecular motors with crown-ether-based host-guest chemistry in a system that functions as photo-responsive host with switchable, multiple and reversible chiral guest recognition. (Figure 1) A series of motorized macrocycles was synthesized by intramolecular cyclization of first-generation molecular motors with oligoethylene glycol chains. Studying different oligoethylene glycol chain lengths, it was established that the incorporation of the motor unit into the macrocycle offers a robust way to simultaneously enable the photochemically driven rotation of the embedded molecular motors without compromising their unidirectional rotary motion and formation of multiple states as well as effective host-guest binding. Notably, the proper size of the macrocycle allows the movement of one half of the core motor unit to pass unhindered through the macrocyclic ring during the 360 degree rotary cycle. An important feature is that the enantiopure motorized macrocycles exhibit distinct chiral states and excellent stereoselectivity with chiral guest molecules. Combined with the ability of the motorized macrocycles to invert chirality by an external trigger (i.e. light or heat), this unique host-guest system controlled by molecular motors can be a starting point to design more complex mechanically interlocked molecules and functional molecular machines.

Results and Discussion

The motorized macrocycles, that is, the host molecules, were designed with a first-generation molecular motor core (Figure 1 a). Functionalization with ethylene glycol chains of different lengths formed various crown-ether rings by one-pot intramolecular etherification-cyclization reactions. The synthesis is summarized in the Supporting Information, Scheme S1. Specifically, the diphenol motor, that is, stable-*cis/trans*-2, was reacted with ethylene glycol ditosylates in the presence of cesium carbonate in acetonitrile to afford stable-*cis/trans* motorized macrocycles (**3**, R₁–R₃, Figure 1 b,c). The yield of the stable-*trans* motorized macrocycle was lower compared to the stable-*cis* one, which might be attributed to the enhanced strain in the *trans* isomer. For example, the yields of stable-*trans*-3 and stable-*cis*-3 were 12% and 54%, respectively. Detailed procedures of the synthesis are provided in the Supporting Information. The molecular structures were fully characterized by ¹H, ¹³C NMR spectroscopies, and high-resolution mass spectrometry (HR-MS; Supporting Information, Figures S50–S71).

The unidirectional rotation of the motorized macrocycles, involving a four-step rotary cycle comprising two photochemical isomerizations and two thermal helix inversion (THI) steps (Figure 1 b), were studied by UV/Vis absorption and ¹H NMR spectroscopies (Figure 2 a–d, for more details, see Figures S1–S3). A tetrahydrofuran (THF) solution of stable-*cis*-3 showed a distinctive absorption peak at 320 nm (Figure 2 a), which red-shifted to 340 nm upon irradiation (310 nm) at –60°C for 1 h with a clear isobestic point (Figure 2 a; Supporting Information, Figure S1a), revealing

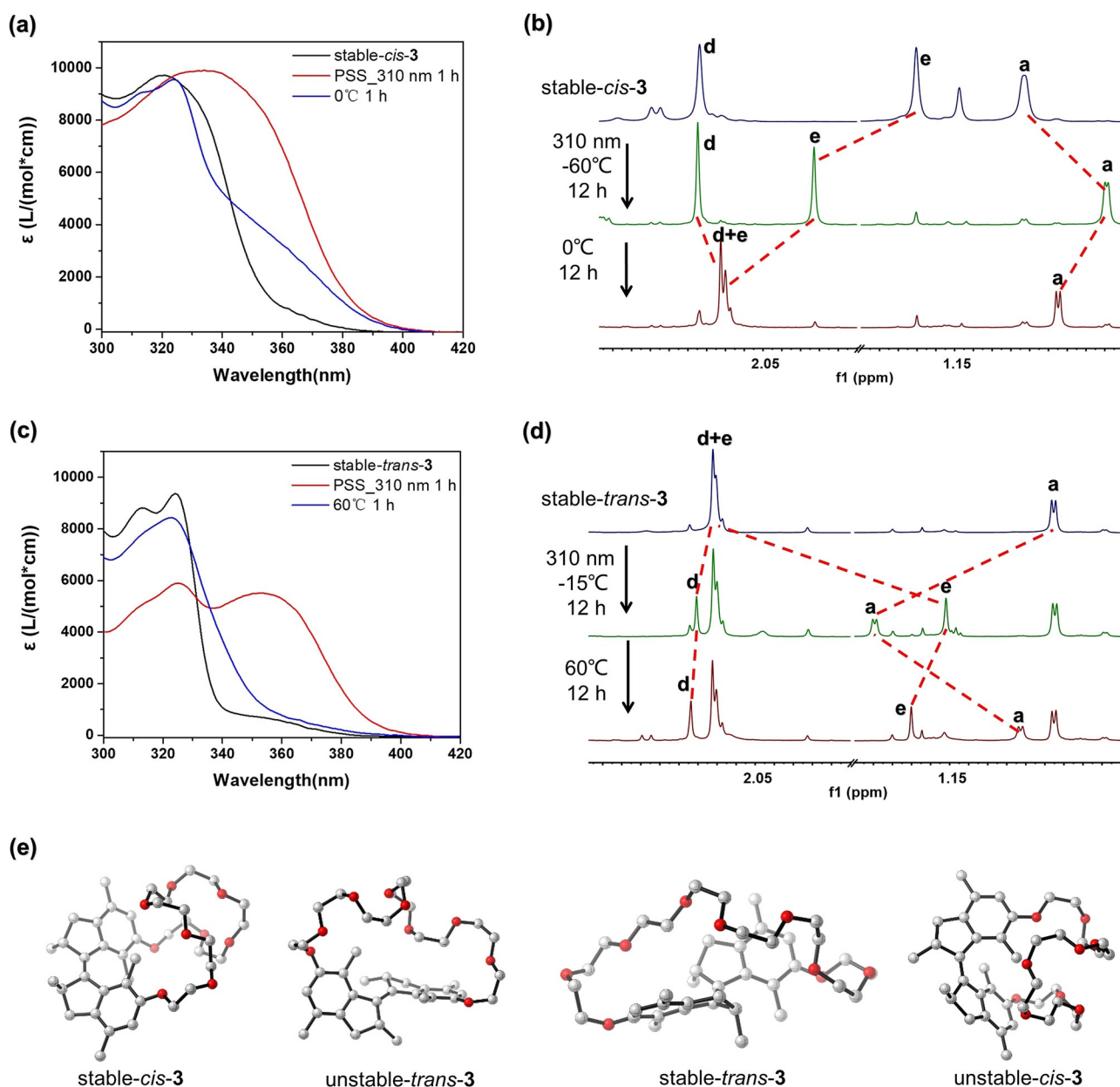


Figure 2. a) UV/Vis absorption spectra of stable-*cis*-**3** after the photoisomerization and THI processes (THF). b) Partial ^1H NMR spectra of stable-*cis*-**3** (600 MHz, 203 K, CD_2Cl_2 , 5 mM) during the photoisomerization and THI processes. c) UV/Vis absorption spectra of stable-*trans*-**3** during the photoisomerization and THI processes (THF). d) Partial ^1H NMR spectra of stable-*trans*-**3** (600 MHz, 203 K, CD_2Cl_2 , 5 mM) during the photoisomerization and THI processes. For the proton assignment, see Figure 1 b. e) The energy minimized optimized geometries of motorized macrocycle **3**.

the selective photoisomerization from stable-*cis*-**3** to unstable-*trans*-**3**.^[22] The resulting solution was heated at 0°C for 1 h, leading to decreased absorption at 330–400 nm (Figure 2a; Supporting Information, Figure S1b), which indicated the effective transformation from unstable-*trans*-**3** to stable-*trans*-**3** via the THI step.^[23]

The isomerization process from stable-*cis*-**3** to stable-*trans*-**3** was furthermore followed by ^1H NMR by irradiating the CD_2Cl_2 solution of stable-*cis*-**3** (310 nm, –60°C, 12 h), and then performing the subsequent THI process at 0°C for 12 h (Figure 2b; Supporting Information, Figure S2a–c). Distinctive proton shifts upon photoisomerization were observed in

the ^1H NMR spectra of the synthetically pure stable-*cis*-**3** upon 310 nm irradiation. The downfield shift of protons H_e ($\Delta\delta = +0.662$ ppm) and upfield shift of the methyl protons H_a ($\Delta\delta = -0.218$ ppm) indicated the successful transformation of the stable-*cis*-**3** to the unstable-*trans*-**3** with a photostationary state (PSS) ratio of 86:14 (unstable-*trans*:stable-*cis*). The resulting unstable-*trans*-**3** can be quantitatively converted to stable-*trans*-**3** via the THI step with a characteristic set of proton shifts, i.e., H_a shifts from $\delta = 0.749$ ppm to 0.879 ppm, and H_e shifts from $\delta = 1.914$ ppm to 2.150 ppm (Figure 2b, Figure S2b,c). The thermal parameters of the transformation from unstable-*trans*-**3** to stable-*trans*-**3** were determined by

Table 1: Kinetic and thermodynamic data.

	ΔG^{\ddagger} [kJ mol ⁻¹]	$t_{1/2}$ at 20 °C
unstable- <i>trans</i> - 3	88.8	12.6 min
unstable- <i>cis</i> - 3	100.3	1.0 d
unstable- <i>trans</i> - R ₃	89.4	16.0 min
unstable- <i>cis</i> - R ₃	106.0	11.2 d

[a] The Gibbs free energy of activation (ΔG), analysis of these data using the Eyring equation ($\Delta G = RT[\ln(k_B/h) - \ln(k/T)]$, where R , h and k_B correspond to the gas, Planck and Boltzmann constants, respectively. The rate constants k of the first-order decay at different temperatures were obtained using the equation $A/A^0 = e^{-kt}$ by UV/Vis absorption changes at 360 nm.

Eyring analysis, which shows the Gibbs free energy of activation ($\Delta G = 88.8$ kJ mol⁻¹), corresponding to a half-life of 12.6 min at 20 °C (Table 1; Supporting Information, Figure S4a), typical for related first-generation motors.^[24]

The subsequent two-step transformation from stable-*trans*-**3** to stable-*cis*-**3** was also followed using UV/Vis and ¹H NMR spectroscopy. After irradiating the THF solution of the purified stable-*trans*-**3** (310 nm, -15 °C), a new absorption band appears at around 360 nm (Figure 2c; Supporting Information, Figure S1c). Meanwhile, proton H_a shifts downfield from $\delta = 0.882$ ppm to 1.352 ppm, accompanying with an upfield shift of proton H_c from $\delta = 2.153$ ppm to 1.160 ppm, in a CD₂Cl₂ solution of the stable-*trans*-**3**, demonstrating the photochemical formation of unstable-*cis*-**3** (PSS ratio 47:53 (unstable-*cis*:stable-*trans*); Figure 2d; Supporting Information, Figure S3a,b).^[21a] Subsequently, heating of the resulting solutions resulted in the bleaching at 360 nm in the UV/Vis spectra (Figure 2c; Supporting Information, Figure S1d) as well as an upfield shift of the methyl proton H_a ($\Delta\delta = -0.383$ ppm) and a downfield shift of H_c ($\Delta\delta = +0.091$ ppm) in the ¹H NMR spectra. These observations are in accordance with the transformation from unstable-*cis*-**3** to stable-*cis*-**3** (Figure 2d; Supporting Information, Figure S3b,c). Utilizing the Eyring analysis, the Gibbs free energy of activation from unstable-*cis*-**3** to stable-*cis*-**3** was determined as $\Delta G = 100.3$ kJ mol⁻¹, corresponding to a half-life of 1.0 d at 20 °C (Table 1; Supporting Information, Figure S4b). Combining all experimental data, it can be concluded that the unidirectional rotation capability in the macrocycles *trans*-/*cis*-**3** motor is fully maintained.

To better understand the structure of these macrocycles, we optimized the structures of the ground state minima of all isomers of macrocycle **3** (reflecting the four states in the rotary cycle) at the PW6B95D3/def2-SVP level of theory, modelling the DCM contribution with the implicit SMD solvation method (Figure 2e). The geometries, subject to the DFT analysis, were preliminarily screened with a conformational analysis (for details, see the Supporting Information). The dihedral angle (θ) of the benzene ring in the molecular motor unit was determined (Supporting Information, Table S1). As expected, the *cis* isomers bear smaller dihedral angles (7.8° for stable-*cis*-**3** vs. 159.4° for stable-*trans*-**3**), allowing the flexible crown ethers to form an accessible semicircular structure which might facilitate the noncovalent recognition with the guest. The distance between the pair of

aryl-methyl protons H_c in the *cis* isomer was relatively small (3.48 Å in the stable *cis* form vs. 5.91 Å in stable-*trans*-**3**), which was consistent with the upfield shift of these protons after photoisomerization of **3** from the stable-*trans* isomer to unstable-*cis* isomer.

Several reference molecules, including *cis*-/*trans*-**R**₁, *cis*-**R**₂ and *cis*-/*trans*-**R**₃, were designed to understand how the presence of the macrocycle affects the rotation properties of the motors (for details, see the Supporting Information). These include an acyclic structure with pending ethylene glycols (**R**₁) and cyclic analogues with different ring sizes (**R**₂, **R**₃). The reference compounds *trans*-/*cis*-**R**₁ and *trans*-/*cis*-**R**₃ exhibited consistent unidirectional rotation capability, as confirmed by similar spectral variations observed in ¹H NMR and UV/Vis studies (Supporting Information, Schemes S2,S3, Figure S5–S9) as with the parent motor **3**. Compared to motorized macrocycle **3**, **R**₃ functionalized with a shorter glycol chain, that is, a hexaethylene glycol, showed a higher Gibbs free energy of activation, which corresponded to a longer half-life of the unstable isomer and slower THI steps (Table 1; Supporting Information, Figure S10). When the molecular motor was functionalized with a triethylene glycol chain, that is, motorized macrocycle **R**₂, the stable-*cis* isomer was obtained, while the cyclization reaction of stable-*trans*-**2** with triethylene glycol chain was inhibited as indicated by the absence of corresponding products in ESI-MS (Supporting Information, Figure S65). The absorption band of stable-*cis*-**R**₂ also exhibited a red-shift when irradiated with 310 nm light, while the absorption band quickly recovered at room temperature (Supporting Information, Figure S11). The ¹H NMR spectra showed no signal change (Supporting Information, Figure S12) owing to the fast recovery. A single-crystal structure of *cis*-**R**₂ (Supporting Information, Figure S13, for more details, see Table S2)^[31] showed that the dihedral angle (θ) between rotor and stator was only 42.7°, indicating that **R**₂ may be locked in the *cis* configurations due to the short crown-ether ring. Combining all data, it can be concluded that the larger macrocyclic motors **3** and **R**₃ perform uncompromised unidirectional rotations.

The host–guest chemistry of crown ethers is well-established, and among the family of guest molecules for crown ethers, ammonium salts are remarkably versatile because of their high-affinity mediated by hydrogen bonds and ion-dipole interactions.^[25] Hence, two ammonium salts, **G1** and **G2** (Figure 1d), were chosen as guest molecules to investigate the host–guest recognition with the motorized macrocycles. Upon addition of **G1**, characteristic proton shifts are observed in the ¹H NMR spectra of stable-*cis*-**3** ([D₆]acetone solution, Figure 3b).^[26] Proton H_f of stable-*cis*-**3** shifted upfield with $\Delta\delta$ of -0.119 ppm (Supporting Information, Figure S14). Protons H_{Ar} and H_I exhibited strong coupling with protons H_{crown ether}, as evident from the two-dimensional nuclear Overhauser effects spectroscopy (NOESY; Supporting Information, Figure S15a). Moreover, a base peak at $m/z = 880.5356$, corresponding to the [stable-*cis*-**3** ⊃ **G1**] ion, was observed in the ESI spectra (Supporting Information, Figure S15b). The results demonstrate the formation of the host–guest system [stable-*cis*-**3** ⊃ **G1**]. To quantify the binding ratio and binding constant (K_b) of this host–guest system, a stable-*cis*-**3** solution

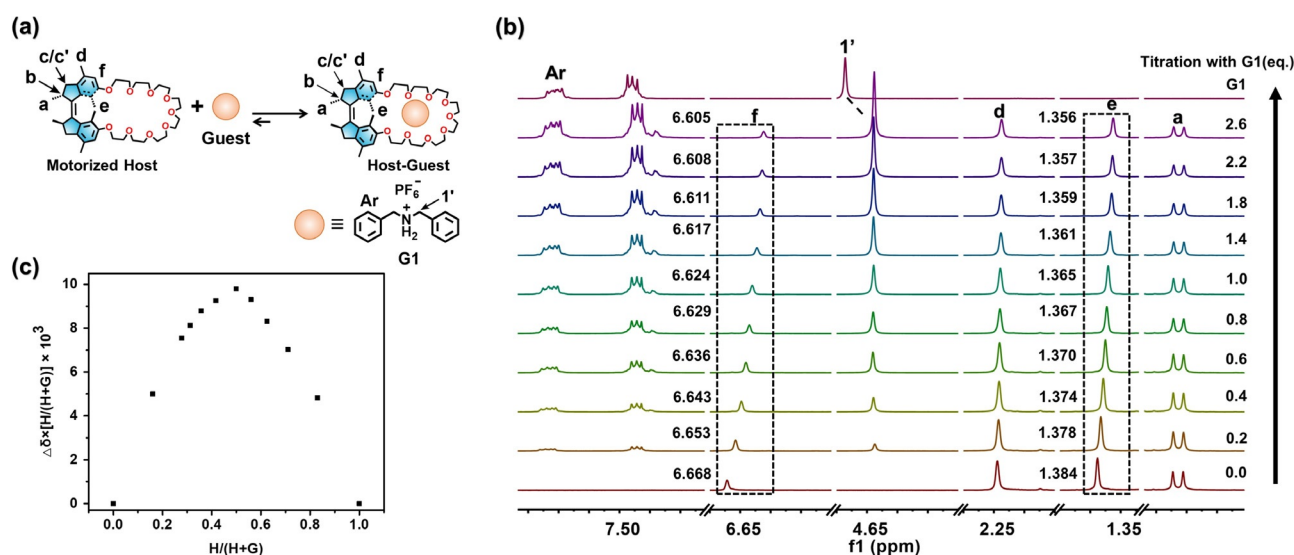


Figure 3. a) Representation of the guest recognition. b) Partial ^1H NMR spectra of stable-*cis*-**3** (5 mM, 400 MHz, 293 K, $[\text{D}_6]$ acetone) upon the stepwise addition of **G1** and c) Job's plot based on the proton shift of H_f in $[\text{D}_6]$ acetone.

was titrated with increasing equivalents of **G1** and followed by ^1H NMR spectroscopy.^[27] The binding ratio between stable-*cis*-**3** and the guest **G1** was determined as 1:1 by Job's plot analysis^[28] (Figure 3b,c; Supporting Information, Figure S15c). An approximate value of $K_a = 219.0 \text{ M}^{-1}$ was obtained by varying the ratio of stable-*cis*-**3** with respect to **G1** in $[\text{D}_6]$ acetone (Figure 3b, for more details, see the Supporting Information, Figure S15c). On the other hand, when guest **G1** was added to the stable-*trans*-**3** solution under identical conditions, no proton shift or typical m/z peak for the complex was observed in the ^1H NMR and mass spectra (Supporting Information, Figure S16), indicating the absence of sufficiently strong host-guest interactions between **G1** and *trans*-**3**. Based on the optimized geometries (Figure 2e; Supporting Information, Table S1), the distinctive difference in binding affinity between *trans*-**3** and *cis*-**3** with **G1** can be attributed to the conformation change of crown ether. The crown ether part of *trans*-**3** is stretched into a more linear conformation, which is obviously disadvantageous for the cavity formation of the crown ether unit essential for guest binding.

Similar to **3**, $[\text{stable-}i\text{-cis-}\mathbf{R}_3 \supset \mathbf{G1}]$ was obtained in $[\text{D}_6]$ acetone with a binding constant K_a of 162.4 M^{-1} , and the HRMS showed a major peak of the host-guest system at $m/z = 792.4838$ (Supporting Information, Figure S17). In contrast, the binding constant of stable-*trans*-**R**₃ was less than 1 M^{-1} (Supporting Information, Figure S18). The binding constants of these macrocycles (**3**, **R**₂ and **R**₃) with the guest **G2** were also obtained (Table 2, for details, see the Supporting

Table 2: Binding constants of guests to the macrocycles (K_a , M^{-1} in $[\text{D}_6]$ acetone).

Guests	Host Macrocycles				
	<i>cis</i> - 3	<i>trans</i> - 3	<i>cis</i> - R ₃	<i>trans</i> - R ₃	<i>cis</i> - R ₂
G1	219.0	<1	162.4	<1	<1
G2	28.3	<1	48.8	<1	<1

Information, Figure S19–S23). These results clearly demonstrated significant differences in the host-guest recognition of the motorized macrocycles between *cis* and *trans* isomers, indicating the possibility of in situ guest capture or release by changing the geometrical configurations of the motorized macrocycles.

The rotation of the motorized macrocycles accessing multiple states in the host-guest system is essential to obtain the in situ dynamic guest capture or release controlled by external light and heat stimuli. In previous studies, we showed that substituents in the molecular motor might affect its motion owing to the presence of intramolecular interactions.^[29] To study how the guest combination affects the rotation ability of the macrocyclic motors, structural changes of $[\text{stable-}i\text{-cis-}\mathbf{3} \supset \mathbf{G1}]$ upon irradiation and heating were investigated by UV/Vis and ^1H NMR spectroscopy (Figure 4; for more details, see the Supporting Information, Figures S24–S27).

The host-guest system of $[\text{stable-}i\text{-cis-}\mathbf{3} \supset \mathbf{G1}]$ in $[\text{D}_6]$ acetone was irradiated with 310 nm light at -60°C for 12 h, leading to the noticeable downfield shifts of protons H_f ($\Delta\delta = +0.048 \text{ ppm}$) and H_e ($\Delta\delta = +0.721 \text{ ppm}$) and upfield shifts of protons H_f ($\Delta\delta = -0.099 \text{ ppm}$) and H_a ($\Delta\delta = -0.249 \text{ ppm}$) in ^1H NMR spectra (Figure 4c, Figure S25). Subsequently, after heating the system in the dark at 0°C for 12 h, protons H_f , H_f , H_e and H_a shifted downfield with $\Delta\delta$ of $+0.069 \text{ ppm}$, $+0.115 \text{ ppm}$, $+0.145 \text{ ppm}$, and $+0.277 \text{ ppm}$, respectively (Figure 4c; Supporting Information, Figure S25). The proton shifts of H_d , H_e and H_a indicated the transformations from stable-*cis*-**3** to unstable-*trans*-**3** and subsequently stable-*trans*-**3** in the $[\text{stable-}i\text{-cis-}\mathbf{3} \supset \mathbf{G1}]$ upon irradiation followed by heating (Figure 4c; Supporting Information, Figure S25). Meanwhile, the proton shifts of H_f and H_f suggested the release of guest **G1** (Figure 4c; Supporting Information, Figure S25), retaining the spectrum of *trans*-**3** (no guest binding). The spectral variations in the UV/Vis spectra (Figure 4b) were consistent with those in

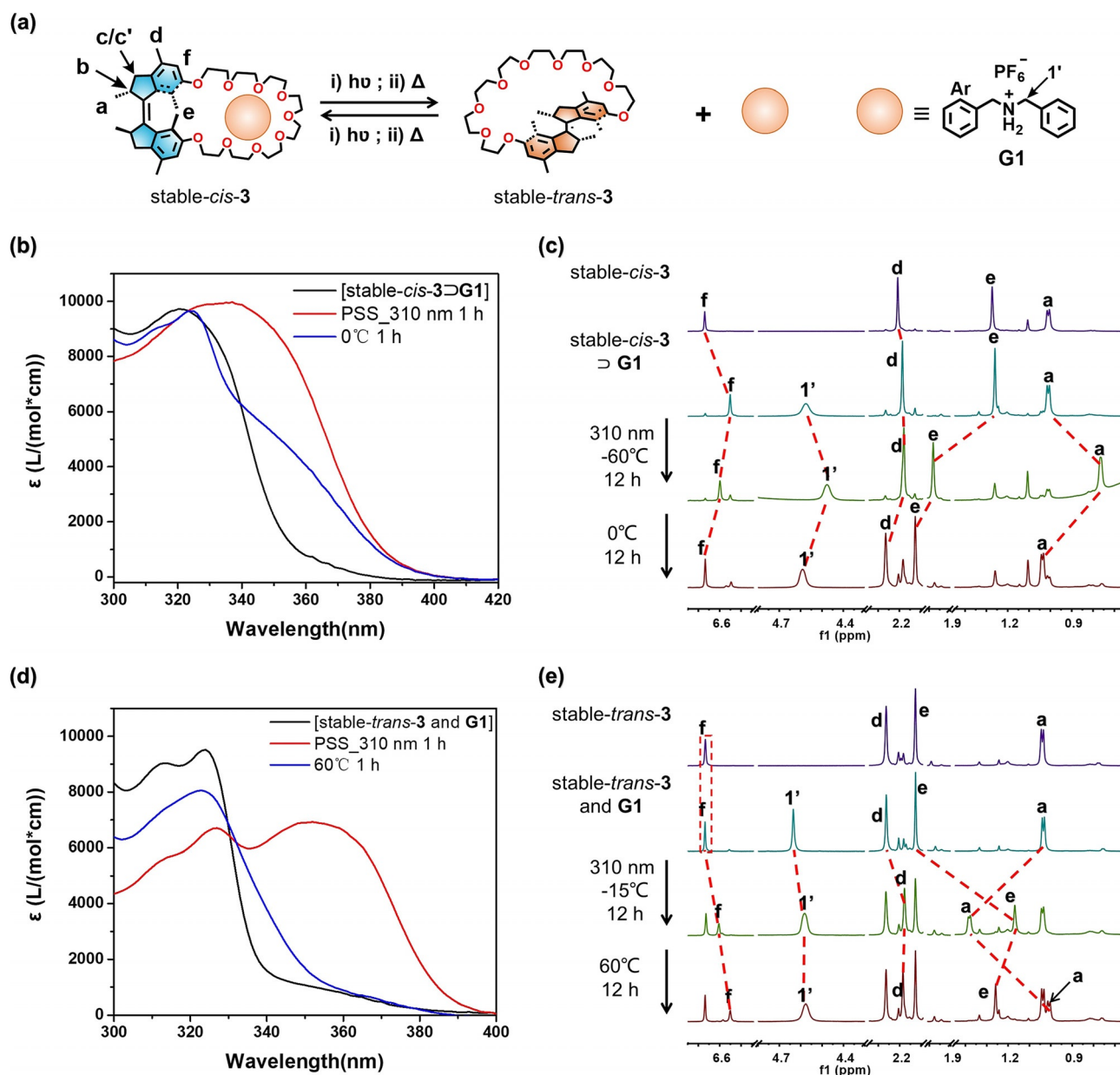


Figure 4. a) Representation of the guest capturing/releasing procedures of motorized macrocycle **3**. b) UV/Vis absorption spectra of the host-guest system before/after photo- and thermal isomerization (THF): from [stable-cis-3 ⊃ G1] to [stable-trans-3 and G1]. c) Partial ¹H NMR spectra during the isomerization processes of the host-guest system (600 MHz, 203 K, [D₆]acetone, 5 mM), starting from [stable-cis-3 ⊃ G1]. d) UV/Vis absorption spectra of the host-guest system before/after photo- and thermal isomerization (THF): from [stable-trans-3 and G1] to [stable-cis-3 ⊃ G1] and e) partial ¹H NMR spectra during the isomerization processes of the host-guest system (600 MHz, 203 K, [D₆]acetone, 5 mM), starting from [stable-trans-3 and G1].

Figure 2a, further indicating the 180° rotation of motorized macrocycle **3**, that is, from stable-cis-3 to stable-trans-3, after forming the host-guest complex with **G1**. The results demonstrate that stable-cis-3 retained its ability to undergo rotational motion after the formation of [stable-cis-3 ⊃ G1], allowing for the controllable release of the guest **G1**.

To explore photo-controlled guest capture, the 1:1 mixture solution of stable-trans-3 and **G1** was irradiated with 310 nm light at -15°C, followed by heating at 60°C. The structural changes during the photoirradiation and heating processes were also analyzed by ¹H NMR and UV/Vis

spectroscopies. The proton shifts of H_a (from δ = 1.04 ppm to 1.386 ppm and 1.014 ppm) and H_c (from δ = 2.126 ppm to 1.169 ppm and 1.258 ppm) indicate the transformations from stable-trans-3 to unstable-cis-3 and stable-cis-3 (Figure 4e; Supporting Information, Figure S26). Moreover, upfield shifts of proton H_f and H_{1'} revealed the capture of guest **G1** when stable-trans-3 is converted to stable-cis-3 upon photoisomerization and THI processes (Figure 4e; Supporting Information, Figure S26). Through Eyring analysis (Supporting Information, Figure S27), the Gibbs free energy of activation and half-life time of the host-guest system were obtained, as

Table 3: Kinetic and thermodynamic data.

	ΔG [kJ mol ⁻¹]	$t_{1/2}$ at 20 °C
[unstable- <i>cis</i> - 3 \supset G1]	101.3	1.5 d
unstable- <i>trans</i> - 3 mixing with G1	88.9	13.4 min

shown in Table 3. Compared to **3** in the absence of **G1**, slightly higher values of Gibbs free energy of activation and longer half-lives of both unstable-*trans*-**3** in the presence of **G1** and [unstable-*cis*-**3** \supset **G1**] (Table 1 and 3) are seen. These effects may derive from additional hydrogen bonds and ion-dipole interactions.

The unique stereochemistry of the first-generation molecular motors enables chiral transmission and dynamic inversion of chirality.^[21d] To investigate the stereoselective recognition ability of the motor macrocycles, enantiopure motors, (*P, P*)-(*R, R*)-*cis*-**3**, (*M, M*)-(*S, S*)-*cis*-**3**, (*P, P*)-(*R, R*)-*trans*-**3** and (*M, M*)-(*S, S*)-*trans*-**3** were separated by using chiral HPLC (Supporting Information, Figures S28–S30 and S32–S34) and the stereochemistry was confirmed by comparing the CD spectra with those of previous first generation motors reported by our group^[21c,d] (Supporting Information, Figures S31 and S35). Non-symmetric dibenzylamine based chiral ammonium salts, **G3**(*R*) and **G3**(*S*), were used as chiral guest molecules. (For details, see the Supporting Information). Base peaks at $m/z = 894.5521$ and $m/z = 894.5519$ in the ESI mass spectra (Supporting Information, Figures S36a and S38a), corresponding to the [(*P, P*)-(*R, R*)-*cis*-**3** \supset **G3**(*R*)] and [(*P, P*)-(*R, R*)-*cis*-**3** \supset **G3**(*S*)] ions, respectively, indicated the formation of host–guest complexes between (*P, P*)-(*R, R*)-*cis*-**3** and the chiral guests. Moreover, the addition of **G3**(*R*) and **G3**(*S*), a CD₂Cl₂ solution (*P, P*)-(*R, R*)-*cis*-**3** showed upfield shifts of protons H_f, H_d and H_e (Supporting Information, Figures S37 and S39), which further confirms the formation of host–guest binding similar to the binding of **G1** (see Figure 3). The binding constants ($K_{R/S}$) between (*P, P*)-(*R, R*)-*cis*-**3** and chiral ammonium salts of **G3**(*R/S*) were determined by ¹H NMR titrations in CD₂Cl₂. Job's plot^[27,28] analysis based on ¹H NMR titrations, showing $H/(H+G) = 0.5$, indicating that the ratio of (*P, P*)-(*R, R*)-*cis*-**3** with both guests **G3**(*R*) and **G3**(*S*) was 1:1 (Supporting Information, Figures S36b and S38b). By fitting the titration data to a 1:1 binding model, binding constants K_R of 2967.4 M⁻¹ and K_S of 5119.8 M⁻¹ were obtained, revealing that the chiral motorized macrocycle (*P, P*)-(*R, R*)-*cis*-**3** exhibited selectivity for preferred binding of the (*S*)-enantiomer ($K_S/K_R = 1.7$; Table 4). Additionally, the simulated Gibbs free energies for the host–guest binding between (*P, P*)-(*R, R*)-*cis*-**3** and the chiral guests, further showed the binding preference of the host with **G3**(*S*) over **G3**(*R*) ($\Delta G = 6.3$ kJ mol⁻¹ at the SMD(DCM)-PW6B95D3/

Table 4: Binding constants of chiral guests to the macrocycle **3** (K_R , K_S , M⁻¹ in CD₂Cl₂).

	(<i>P, P</i>)-(<i>R, R</i>)- <i>cis</i> - 3	(<i>M, M</i>)-(<i>R, R</i>)- <i>cis</i> - 3	(<i>P, P</i>)-(<i>R, R</i>)- <i>trans</i> - 3
G3 (<i>R</i>)	2967.4	974.0	138.5
G3 (<i>S</i>)	5119.8	386.5	78.2

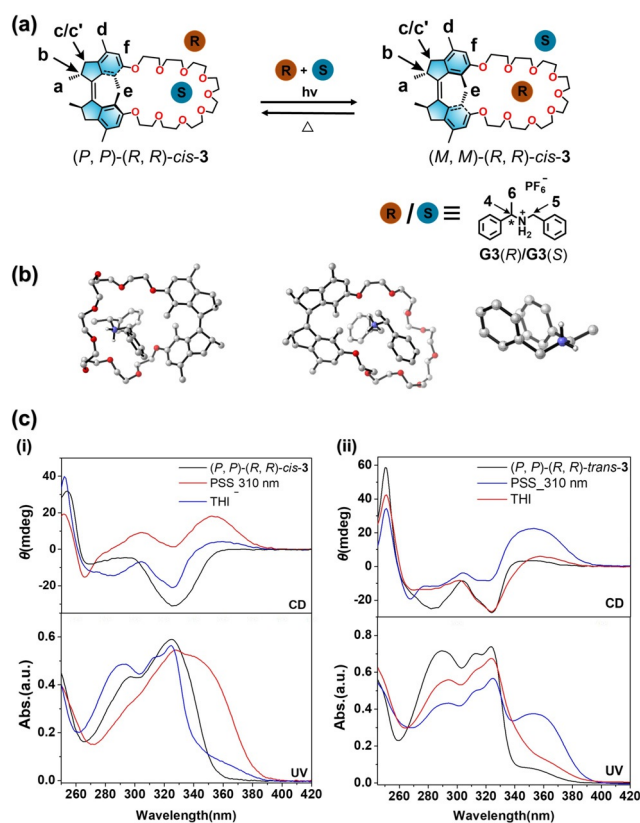


Figure 5. a) Representation of stereoselective guest recognition. b) B3LYP/6-31G++(d,p) optimized geometries of [(*P, P*)-(*R, R*)-*cis*-**3** \supset **G3**(*R*)] (left), [(*P, P*)-(*R, R*)-*cis*-**3** \supset **G3**(*S*)] (middle) and **G3**(*R*) (right). c) (i) CD (upper) and UV/Vis absorption (lower) spectra of (*P, P*)-(*R, R*)-*cis*-**3** (55 μM in CH₂Cl₂) before and after photoisomerization and THI: from (*P, P*)-(*R, R*)-*cis*-**3** to (*P, P*)-(*R, R*)-*trans*-**3**, (ii) CD and UV/Vis absorption spectra of (*P, P*)-(*R, R*)-*trans*-**3** (75 μM in CH₂Cl₂) before and after photoisomerization and THI: from (*P, P*)-(*R, R*)-*trans*-**3** to (*P, P*)-(*R, R*)-*cis*-**3**.

def2-SVP level of theory (Figure 5 b; Supporting Information, Table S9).

On the other hand, (*P, P*)-(*R, R*)-*trans*-**3** exhibited a poor binding affinity with the chiral guest (Table 4, for details, see the Supporting Information, Figures S40, S41). To determine the binding constant for **G3**(*R/S*) with (*M, M*)-(*R, R*)-*cis*-**3**,^[30] competitive titrations to the PSS mixture (PSS₃₁₀; (*M, M*)-(*R, R*)-*cis*:(*P, P*)-(*R, R*)-*trans* = 40:60) were carried out under the same conditions. It was found that now the (*R*)-enantiomer of **G3** binds stronger ($K_R/K_S = 2.5$; Table 4, for details, see the Supporting Information, Figures S42, 43). Owing to the dynamic chirality inversion of helicity of the motor macrocycle (*P, P*)-(*R, R*)-*cis*-**3** to (*P, P*)-(*R, R*)-*trans*-**3** (*M, M*)-(*R, R*)-*cis*-**3** upon photochemical and thermal isomerization steps (Figure 5 c), this unique chiral host **3** can modulate its binding affinity and stereoselectivity (*R* or *S*) for different enantiomers of the chiral guest.

Conclusion

In summary, we have successfully merged photochemically-driven molecular motors with the host–guest chemistry

of crown ether. The unidirectional rotation motion of molecular motors is maintained in the macrocyclic system depending on the ring size. The photoisomerization process enables the reversible modulation of the conformation of the crown ether moiety, leading to distinct photo-switchable binding affinity with dialkylammonium guest molecules. Furthermore, the modulation of chiral recognition has been realized using the enantiopure motor macrocycle and the enantioselectivity of the chiral guest binding can be dynamically inverted by the unidirectional rotation of the motor macrocycle. We foresee that this unprecedented combination of molecular motors, macrocyclic host–guest chemistry, enabling multiple interconvertible helical states and distinct receptor structures, will be an excellent starting point for the design and construction of motorized macrocycles and more complex artificial molecular switches and machines.

Acknowledgements

This work was supported by the National Natural Science Foundation of China (grants 22025503, 21790361, 21871084, and 21672060), Shanghai Municipal Science and Technology Major Project (grant 2018SHZDZX03), the Fundamental Research Funds for the Central Universities, the Programme of Introducing Talents of Discipline to Universities (grant B16017), Program of Shanghai Academic/Technology Research Leader (19XD1421100), the Shanghai Science and Technology Committee (grant 17520750100). This project has received funding from the European Union's Horizon 2020 research and innovation programme under the Marie Skłodowska Curie grant agreement (Q. Zhang: individual fellowship No. 101025041; S. Crespi: individual fellowship No. 838280). B.L.F. acknowledges financial support from the European Research Council (ERC; advanced grant No.694345 to B.L.F.) and the Dutch Ministry of Education, Culture and Science (Gravitation program No.024.001.035). We thank the Research Center of Analysis and Test of East China University of Science and Technology for help on the characterization.

Conflict of interest

The authors declare no conflict of interest.

Keywords: capture and release · host–guest interactions · motorized macrocycles · photo-responsiveness · stereoselectivity

- [1] a) D. J. Cram, *Angew. Chem. Int. Ed. Engl.* **1988**, *27*, 1009–1020; *Angew. Chem.* **1988**, *100*, 1041–1052; b) J.-M. Lehn, *Angew. Chem. Int. Ed. Engl.* **1988**, *27*, 89–112; *Angew. Chem.* **1988**, *100*, 91–116; c) C. J. Pedersen, *Angew. Chem. Int. Ed. Engl.* **1988**, *27*, 1021–1027; *Angew. Chem.* **1988**, *100*, 1053–1059.
- [2] a) D. J. Cram, J. M. Cram, *Science* **1974**, *183*, 803; b) J. Rebek, Jr., *Chem. Commun.* **2000**, 637–643; c) A. Harada, Y. Takashima, H. Yamaguchi, *Chem. Soc. Rev.* **2009**, *38*, 875–882; d) S. J. Barrow, S. Kaser, M. J. Rowland, J. Del Barrio, O. A.

- Scherman, *Chem. Rev.* **2015**, *115*, 12320–12406; e) Z. Liu, S. K. M. Nalluri, J. F. Stoddart, *Chem. Soc. Rev.* **2017**, *46*, 2459–2478; f) X. Ji, M. Ahmed, L. Long, N. M. Khashab, F. Huang, J. L. Sessler, *Chem. Soc. Rev.* **2019**, *48*, 2682–2697.
- [3] a) S. T. J. Ryan, J. del Barrio, R. Suardíz, D. F. Ryan, E. Rosta, O. A. Scherman, *Angew. Chem. Int. Ed.* **2016**, *55*, 16096–16100; *Angew. Chem.* **2016**, *128*, 16330–16334; b) X. Chi, W. Cen, J. A. Queenan, L. Long, V. M. Lynch, N. M. Khashab, J. L. Sessler, *J. Am. Chem. Soc.* **2019**, *141*, 6468–6472; c) Z. Ye, Z. Yang, L. Wang, L. Chen, Y. Cai, P. Deng, W. Feng, X. Li, L. Yuan, *Angew. Chem. Int. Ed.* **2019**, *58*, 12519–12523; *Angew. Chem.* **2019**, *131*, 12649–12653.
- [4] a) V. Balzani, A. Credi, F. M. Raymo, J. F. Stoddart, *Angew. Chem. Int. Ed.* **2000**, *39*, 3348–3391; *Angew. Chem.* **2000**, *112*, 3484–3530; b) W. R. Browne, B. L. Feringa, *Nat. Nanotechnol.* **2006**, *1*, 25–35; c) A. Cnossen, W. R. Browne, B. L. Feringa, *Top. Curr. Chem.* **2014**, *354*, 139–162; d) S. Erbas-Cakmak, D. A. Leigh, C. T. McTernan, A. L. Nussbaumer, *Chem. Rev.* **2015**, *115*, 10081–10206; e) B. L. Feringa, *Angew. Chem. Int. Ed.* **2017**, *56*, 11060–11078; *Angew. Chem.* **2017**, *129*, 11206–11226; f) J.-P. Sauvage, *Angew. Chem. Int. Ed.* **2017**, *56*, 11080–11093; *Angew. Chem.* **2017**, *129*, 11228–11242; g) J. F. Stoddart, *Angew. Chem. Int. Ed.* **2017**, *56*, 11094–11125; *Angew. Chem.* **2017**, *129*, 11244–11277; h) D. Dattler, G. Fuks, J. Heiser, E. Moulin, A. Perrot, X. Yao, N. Giuseppone, *Chem. Rev.* **2020**, *120*, 310–433; i) A. S. Braegelman, M. J. Webber, *Theranostics* **2019**, *9*, 3017–3040; j) V. García-López, D. Liu, J. M. Tour, *Chem. Rev.* **2020**, *120*, 79–124; k) L.-L. Wang, M. Quan, T.-L. Yang, Z. Chen, W. Jiang, *Angew. Chem. Int. Ed.* **2020**, *59*, 23817–23824; *Angew. Chem.* **2020**, *132*, 24025–24032; l) Q. Wang, Q. Zhang, Q.-W. Zhang, X. Li, C.-X. Zhao, T.-Y. Xu, D.-H. Qu, H. Tian, *Nat. Commun.* **2020**, *11*, 158; m) P. Wei, X. Zhang, J. Liu, G.-G. Shan, H. Zhang, J. Qi, W. Zhao, H. H. Y. Sung, I. D. Williams, J. W. Y. Lam, B. Z. Tang, *Angew. Chem. Int. Ed.* **2020**, *59*, 9293–9298; *Angew. Chem.* **2020**, *132*, 9379–9384; n) D. Xia, P. Wang, X. Ji, N. M. Khashab, J. L. Sessler, F. Huang, *Chem. Rev.* **2020**, *120*, 6070–6123; o) I. Aprahamian, *ACS Cent. Sci.* **2020**, *6*, 347–358.
- [5] a) D.-H. Qu, Q.-C. Wang, Q.-W. Zhang, X. Ma, H. Tian, *Chem. Rev.* **2015**, *115*, 7543–7588; b) J. Murray, K. Kim, T. Ogoshi, W. Yao, B. C. Gibb, *Chem. Soc. Rev.* **2017**, *46*, 2479–2496; c) A. Jana, S. Bähring, M. Ishida, S. Goeb, D. Canvet, M. Sallé, J. O. Jeppesen, J. L. Sessler, *Chem. Soc. Rev.* **2018**, *47*, 5614–5645; d) Z. Li, N. Song, Y.-W. Yang, *Matter* **2019**, *1*, 345–368; e) A. Blanco-Gómez, P. Cortón, L. Barravecchia, I. Neira, E. Pazos, C. Peinador, M. D. García, *Chem. Soc. Rev.* **2020**, *49*, 3834–3862.
- [6] a) B. L. Feringa, W. R. Browne, *Molecular Switches*, 2nd ed., Wiley-VCH, Weinheim, **2011**; b) H. Huang, H. Sato, T. Aida, *J. Am. Chem. Soc.* **2017**, *139*, 8784–8787; c) J. T. Foy, Q. Li, A. Goujon, J.-R. Colard-Itté, G. Fuks, E. Moulin, O. Schiffmann, D. Dattler, D. P. Funeriu, N. Giuseppone, *Nat. Nanotechnol.* **2017**, *12*, 540–545; d) C. Nacci, M. Baroncini, A. Credi, L. Grill, *Angew. Chem. Int. Ed.* **2018**, *57*, 15034–15039; *Angew. Chem.* **2018**, *130*, 15254–15259; e) W. Cullen, H. Takezawa, M. Fujita, *Angew. Chem. Int. Ed.* **2019**, *58*, 9171–9173; *Angew. Chem.* **2019**, *131*, 9269–9271; f) M. Baroncini, S. Silvi, A. Credi, *Chem. Rev.* **2020**, *120*, 200–268; g) H. Wu, Y. Chen, X. Dai, P. Li, J. F. Stoddart, Y. Liu, *J. Am. Chem. Soc.* **2019**, *141*, 6583–6591; h) A. B. Grommet, L. M. Lee, R. Klajn, *Acc. Chem. Res.* **2020**, *53*, 2600–2610; i) Z.-T. Shi, Y.-X. Hu, Z. Hu, Q. Zhang, S.-Y. Chen, M. Chen, J.-J. Yu, G.-Q. Yin, H. Sun, L. Xu, X. Li, B. L. Feringa, H.-B. Yang, H. Tian, D.-H. Qu, *J. Am. Chem. Soc.* **2021**, *143*, 442–452.
- [7] a) D. Samanta, J. Gemen, Z. Chu, Y. Diskin-Posner, L. J. W. Shimon, R. Klajn, *Proc. Natl. Acad. Sci. USA* **2018**, *115*, 9379; b) G. Ragazzon, M. Baroncini, S. Silvi, M. Venturi, A. Credi, *Nat. Nanotechnol.* **2015**, *10*, 70–75; c) K. Iwasa, Y. Takashima, A. Harada, *Nat. Chem.* **2016**, *8*, 625–632; d) H. Wu, Y. Chen, L.

- Zhang, O. Anamimoghadam, D. Shen, Z. Liu, K. Cai, C. Pezzato, C. L. Stern, Y. Liu, J. F. Stoddart, *J. Am. Chem. Soc.* **2019**, *141*, 1280–1289; e) Y. Liu, H. Wang, P. Liu, H. Zhu, B. Shi, X. Hong, F. Huang, *Angew. Chem. Int. Ed.* **2021**, *60*, 5766–5770; *Angew. Chem.* **2021**, *133*, 5830–5834; f) M. Kondo, K. Nakamura, C. G. Krishnan, S. Takizawa, T. Abe, H. Sasai, *ACS Catal.* **2021**, *11*, 1863–1867.
- [8] a) S. Shinka, T. Minami, Y. Kusano, O. Manabe, *Tetrahedron Lett.* **1982**, *23*, 2581–2584; b) S. Shinkai, T. Minami, Y. Kusano, O. Manabe, *J. Am. Chem. Soc.* **1983**, *105*, 1851–1856; c) Y. Wang, N. Ma, Z. Wang, X. Zhang, *Angew. Chem. Int. Ed.* **2007**, *46*, 2823–2826; *Angew. Chem.* **2007**, *119*, 2881–2884; d) T. Avellini, H. Li, A. Coskun, G. Barin, A. Trabolsi, A. N. Basuray, S. K. Dey, A. Credi, S. Silvi, J. F. Stoddart, M. Venturi, *Angew. Chem. Int. Ed.* **2012**, *51*, 1611–1615; *Angew. Chem.* **2012**, *124*, 1643–1647; e) M. Baroncini, S. Silvi, M. Venturi, A. Credi, *Angew. Chem. Int. Ed.* **2012**, *51*, 4223–4226; *Angew. Chem.* **2012**, *124*, 4299–4302; f) F. Tian, D. Jiao, F. Biedermann, O. A. Scherman, *Nat. Commun.* **2012**, *3*, 1207; g) X. Chi, X. Ji, D. Xia, F. Huang, *J. Am. Chem. Soc.* **2015**, *137*, 1440–1443; h) H. Zhao, S. Sen, T. Udayabhaskararao, M. Sawczyk, K. Kucanda, D. Manna, P. K. Kundu, J.-W. Lee, P. Král, R. Klajn, *Nat. Nanotechnol.* **2016**, *11*, 82–88; i) Y.-F. Yin, M.-Y. Yun, L. Wu, H.-Y. Duan, X.-M. Jiang, T.-G. Zhan, J. Cui, L.-J. Liu, K.-D. Zhang, *Angew. Chem. Int. Ed.* **2019**, *58*, 12705–12710; *Angew. Chem.* **2019**, *131*, 12835–12840.
- [9] a) D. G. Amirsakis, M. A. Garcia-Garibay, S. J. Rowan, J. F. Stoddart, A. J. P. White, D. J. Williams, *Angew. Chem. Int. Ed.* **2001**, *40*, 4256–4261; *Angew. Chem.* **2001**, *113*, 4386–4391; b) E. J. F. Klotz, T. D. W. Claridge, H. L. Anderson, *J. Am. Chem. Soc.* **2006**, *128*, 15374–15375; c) S. Ikejiri, Y. Takashima, M. Osaki, H. Yamaguchi, A. Harada, *J. Am. Chem. Soc.* **2018**, *140*, 17308–17315.
- [10] a) M. Inouye, M. Ueno, T. Kitao, K. Tsuchiya, *J. Am. Chem. Soc.* **1990**, *112*, 8977–8979; b) K. Kimura, T. Yamashita, M. Yokoyama, *J. Chem. Soc. Chem. Commun.* **1991**, 147–148; c) D. Samanta, D. Galaktionova, J. Gemen, L. J. W. Shimon, Y. Diskin-Posner, L. Avram, P. Král, R. Klajn, *Nat. Commun.* **2018**, *9*, 641; d) L. Kortekaas, W. R. Browne, *Chem. Soc. Rev.* **2019**, *48*, 3406–3424.
- [11] a) M. Takeshita, M. Irie, *Tetrahedron Lett.* **1998**, *39*, 613–616; b) M. Takeshita, M. Irie, *J. Org. Chem.* **1998**, *63*, 6643–6649; c) S. H. Kawai, *Tetrahedron Lett.* **1998**, *39*, 4445–4448; d) S. Fredrich, A. Bonasera, V. Valderrey, S. Hecht, *J. Am. Chem. Soc.* **2018**, *140*, 6432–6440; e) D. E. Williams, C. R. Martin, E. A. Dolgoplova, A. Swifton, D. C. Godfrey, O. A. Ejegbavwo, P. J. Pellechia, M. D. Smith, N. B. Shustova, *J. Am. Chem. Soc.* **2018**, *140*, 7611–7622.
- [12] a) N. Koumura, R. W. J. Zijlstra, R. A. van Delden, N. Harada, B. L. Feringa, *Nature* **1999**, *401*, 152–155; b) N. Koumura, E. M. Geertsema, A. Meetsma, B. L. Feringa, *J. Am. Chem. Soc.* **2000**, *122*, 12005–12006; c) L. Greb, J.-M. Lehn, *J. Am. Chem. Soc.* **2014**, *136*, 13114–13117; d) J. C. M. Kistemaker, P. Štacko, J. Visser, B. L. Feringa, *Nat. Chem.* **2015**, *7*, 890–896; e) A. Faulkner, T. van Leeuwen, B. L. Feringa, S. J. Wezenberg, *J. Am. Chem. Soc.* **2016**, *138*, 13597–13603; f) S. Kassem, T. van Leeuwen, A. S. Lubbe, M. R. Wilson, B. L. Feringa, D. A. Leigh, *Chem. Soc. Rev.* **2017**, *46*, 2592–2621; g) E. Uhl, S. Thumser, P. Mayer, H. Dube, *Angew. Chem. Int. Ed.* **2018**, *57*, 11064–11068; *Angew. Chem.* **2018**, *130*, 11231–11235; h) E. Uhl, P. Mayer, H. Dube, *Angew. Chem. Int. Ed.* **2020**, *59*, 5730–5737; *Angew. Chem.* **2020**, *132*, 5779–5786.
- [13] a) R. Eelkema, M. M. Pollard, J. Vicario, N. Katsonis, B. S. Ramon, C. W. M. Bastiaansen, D. J. Broer, B. L. Feringa, *Nature* **2006**, *440*, 163–163; b) A. Ryabchun, F. Lancia, J. Chen, D. Morozov, B. L. Feringa, N. Katsonis, *Adv. Mater.* **2020**, *32*, 2004420; c) T. Orlova, F. Lancia, C. Loussert, S. Iamsaard, N. Katsonis, E. Brasselet, *Nat. Nanotechnol.* **2018**, *13*, 304–308; d) J. Sun, R. Lan, Y. Gao, M. Wang, W. Zhang, L. Wang, L. Zhang, Z. Yang, H. Yang, *Adv. Sci.* **2018**, *5*, 1700613.
- [14] a) Y. S. Kim, M. Liu, Y. Ishida, Y. Ebina, M. Osada, T. Sasaki, T. Hikima, M. Takata, T. Aida, *Nat. Mater.* **2015**, *14*, 1002–1007; b) Q. Zhang, D.-H. Qu, H. Tian, B. L. Feringa, *Matter* **2020**, *3*, 355–370.
- [15] a) Q. Li, G. Fuks, E. Moulin, M. Maaloum, M. Rawiso, I. Kulic, J. T. Foy, N. Giuseppone, *Nat. Nanotechnol.* **2015**, *10*, 161–165; b) S. J. Wezenberg, C. M. Croisetu, M. C. A. Stuart, B. L. Feringa, *Chem. Sci.* **2016**, *7*, 4341–4346.
- [16] S. Chen, F. K.-C. Leung, M. C. A. Stuart, C. Wang, B. L. Feringa, *J. Am. Chem. Soc.* **2020**, *142*, 10163–10172.
- [17] a) V. García-López, F. Chen, L. G. Nilewski, G. Duret, A. Aliyan, A. B. Kolomeisky, J. T. Robinson, G. Wang, R. Pal, J. M. Tour, *Nature* **2017**, *548*, 567–572; b) S. Chen, Y. Wang, T. Nie, C. Bao, C. Wang, T. Xu, Q. Lin, D.-H. Qu, X. Gong, Y. Yang, L. Zhu, H. Tian, *J. Am. Chem. Soc.* **2018**, *140*, 17992–17998.
- [18] a) A. C. Coleman, J. Areephong, J. Vicario, A. Meetsma, W. R. Browne, B. L. Feringa, *Angew. Chem. Int. Ed.* **2010**, *49*, 6580–6584; *Angew. Chem.* **2010**, *122*, 6730–6734; b) R. A. van Delden, M. K. J. ter Wiel, M. M. Pollard, J. Vicario, N. Koumura, B. L. Feringa, *Nature* **2005**, *437*, 1337–1340.
- [19] a) W. Danowski, T. van Leeuwen, S. Abdolazadeh, D. Roke, W. R. Browne, S. J. Wezenberg, B. L. Feringa, *Nat. Nanotechnol.* **2019**, *14*, 488–494; b) W. Danowski, F. Castiglioni, A. S. Sardjan, S. Krause, L. Pfeifer, D. Roke, A. Comotti, W. R. Browne, B. L. Feringa, *J. Am. Chem. Soc.* **2020**, *142*, 9048–9056.
- [20] a) A. Saywell, A. Bakker, J. Mielke, T. Kumagai, M. Wolf, V. García-López, P.-T. Chiang, J. M. Tour, L. Grill, *ACS Nano* **2016**, *10*, 10945–10952; b) T. Kudernac, N. Ruangsapapichat, M. Parschau, B. Maciá, N. Katsonis, S. R. Harutyunyan, K.-H. Ernst, B. L. Feringa, *Nature* **2011**, *479*, 208–211; c) J.-F. Morin, Y. Shirai, J. M. Tour, *Org. Lett.* **2006**, *8*, 1713–1716.
- [21] a) J. Wang, B. L. Feringa, *Science* **2011**, *331*, 1429; b) S. J. Wezenberg, M. Vlatković, J. C. M. Kistemaker, B. L. Feringa, *J. Am. Chem. Soc.* **2014**, *136*, 16784–16787; c) D. Zhao, T. M. Neubauer, B. L. Feringa, *Nat. Commun.* **2015**, *6*, 6652; d) M. Vlatković, B. L. Feringa, S. J. Wezenberg, *Angew. Chem. Int. Ed.* **2016**, *55*, 1001–1004; *Angew. Chem.* **2016**, *128*, 1013–1016.
- [22] A. S. Lubbe, C. Böhmer, F. Tosi, W. Szymanski, B. L. Feringa, *J. Org. Chem.* **2018**, *83*, 11008–11018.
- [23] a) M. M. Pollard, A. Meetsma, B. L. Feringa, *Org. Biomol. Chem.* **2008**, *6*, 507–512; b) K.-Y. Chen, O. Ivashenko, G. T. Carroll, J. Robertus, J. C. M. Kistemaker, G. London, W. R. Browne, P. Rudolf, B. L. Feringa, *J. Am. Chem. Soc.* **2014**, *136*, 3219–3224; c) J. C. M. Kistemaker, S. F. Pizzolato, T. van Leeuwen, T. C. Pijper, B. L. Feringa, *Chem. Eur. J.* **2016**, *22*, 13478–13487; d) S. F. Pizzolato, B. S. L. Collins, T. van Leeuwen, B. L. Feringa, *Chem. Eur. J.* **2017**, *23*, 6174–6184.
- [24] a) R. W. J. Zijlstra, W. F. Jager, B. de Lange, P. T. van Duijnen, B. L. Feringa, H. Goto, A. Saito, N. Koumura, N. Harada, *J. Org. Chem.* **1999**, *64*, 1667–1674; b) M. K. J. ter Wiel, R. A. van Delden, A. Meetsma, B. L. Feringa, *J. Am. Chem. Soc.* **2003**, *125*, 15076–15086; c) M. K. J. ter Wiel, R. A. van Delden, A. Meetsma, B. L. Feringa, *J. Am. Chem. Soc.* **2005**, *127*, 14208–14222; d) M. K. J. ter Wiel, M. G. Kwit, A. Meetsma, B. L. Feringa, *Org. Biomol. Chem.* **2007**, *5*, 87–96; e) T. van Leeuwen, J. Gan, J. C. M. Kistemaker, S. F. Pizzolato, M.-C. Chang, B. L. Feringa, *Chem. Eur. J.* **2016**, *22*, 7054–7058.
- [25] a) B. L. Allwood, H. Shahriari-Zavareh, J. F. Stoddart, D. J. Williams, *J. Chem. Soc. Chem. Commun.* **1987**, 1058–1061; b) P. R. Ashton, P. J. Campbell, P. T. Glink, D. Philp, N. Spencer, J. F. Stoddart, E. J. T. Chrystal, S. Menzer, D. J. Williams, P. A. Tasker, *Angew. Chem. Int. Ed. Engl.* **1995**, *34*, 1865–1869; *Angew. Chem.* **1995**, *107*, 1997–2001; c) K. Zhu, V. N. Vukotic, C. A. O’Keefe, R. W. Schurko, S. J. Loeb, *J. Am. Chem. Soc.*

- 2014**, 136, 7403–7409; d) C. Biagini, S. D. P. Fielden, D. A. Leigh, F. Schaufelberger, S. Di Stefano, D. Thomas, *Angew. Chem. Int. Ed.* **2019**, 58, 9876–9880; *Angew. Chem.* **2019**, 131, 9981–9985.
- [26] a) E. M. G. Jamieson, S. M. Goldup, *Nat. Chem.* **2019**, 11, 765–767; b) J. Groppi, L. Casimiro, M. Canton, S. Corra, M. Jafari-Nasab, G. Tabacchi, L. Cavallo, M. Baroncini, S. Silvi, E. Fois, A. Credi, *Angew. Chem. Int. Ed.* **2020**, 59, 14825–14834; *Angew. Chem.* **2020**, 132, 14935–14944.
- [27] P. Thordarson, *Chem. Soc. Rev.* **2011**, 40, 1305–1323.
- [28] a) D. Brynn Hibbert, P. Thordarson, *Chem. Commun.* **2016**, 52, 12792–12805; b) J. S. Renny, L. L. Tomasevich, E. H. Tallmadge, D. B. Collum, *Angew. Chem. Int. Ed.* **2013**, 52, 11998–12013; *Angew. Chem.* **2013**, 125, 12218–12234.
- [29] a) D.-H. Qu, B. L. Feringa, *Angew. Chem. Int. Ed.* **2010**, 49, 1107–1110; *Angew. Chem.* **2010**, 122, 1125–1128; b) J.-J. Yu, L.-Y. Zhao, Z.-T. Shi, Q. Zhang, G. London, W.-J. Liang, C. Gao, M.-M. Li, X.-M. Cao, H. Tian, B. L. Feringa, D.-H. Qu, *J. Org. Chem.* **2019**, 84, 5790–5802.
- [30] (*M, M*)-(*R, R*)-*cis*-**3** was generated from (*P, P*)-(*R, R*)-*trans*-**3** by irradiating with 310 nm UV light.
- [31] Deposition Number 2063381 contains the supplementary crystallographic data for this paper. These data are provided free of charge by the joint Cambridge Crystallographic Data Centre and Fachinformationszentrum Karlsruhe Access Structures service www.ccdc.cam.ac.uk/structures.

Manuscript received: March 26, 2021
Revised manuscript received: May 4, 2021
Accepted manuscript online: May 6, 2021
Version of record online: June 15, 2021